ELSEVIER

Journal of Chromatography A, 921 (2001) 109–119

JOURNAL OF CHROMATOGRAPHY A

www.elsevier.com/locate/chroma

Protein adsorption equilibria and kinetics to a poly(vinyl alcohol)-based magnetic affinity support

Bo Xue, Yan Sun*

Department of Biochemical Engineering, Tianjin University, Tianjin 300072, China

Received 19 December 2000; received in revised form 10 April 2001; accepted 10 April 2001

Abstract

A poly(vinyl alcohol)-based magnetic gel entrapping Fe_3O_4 colloids has been prepared by an emulsification-crosslinking method. The gel was modified with Cibacron blue 3GA, and thus a magnetic affinity support was produced. The adsorption equilibrium studies showed that the adsorption isotherm of lysozyme was nearly rectangular, with a capacity of 254 mg/ml, while the adsorption isotherm of bovine serum albumin obeyed the Henry's law. Uptake kinetics of the two proteins was investigated and analyzed with a pore diffusion model and a homogeneous diffusion model. Experimental results showed that the magnetic affinity gel had magnetic responsiveness and favorable properties in protein adsorption, and was mechanically and chemically stable.

Keywords: Adsorption; Kinetic studies; Poly(vinyl alcohol) sorbent; Affinity sorbents; Magnetic sorbents; Proteins

1. Introduction

Chromatography is a powerful technology for the purification of biological substances in both analytical and preparative scales. However, packed-bed chromatographic column is prone to clogging so that the method is unable to process particulate feedstocks such as whole fermentation broth, cell disruptates and unclarified biological extracts. To overcome this drawback, various alternative separation techniques have been developed, including fluidized bed adsorption [1], expanded bed adsorption [2] and magnetic separations [3,4]. The new techniques offer great opportunities for process integration by achieving particulate removal and desired product capture in a single operation.

There have been several separation approaches performed under magnetic field. The most well known technique is the magnetically stabilized fluidized bed [4]. The others involve high gradient magnetic filtration [5], magnetophoresis [6], and magnetic split-flow thin fractionation [7]. These techniques are all based on the magnetic feature of the solid-phase employed to achieve a desired separation operation. Thus, the availability of inexpensive magnetic supports with high selectivity and magnetic responsiveness is crucial to the large-scale application of the above-mentioned techniques.

Currently, several procedures for the preparation of magnetic supports have been attempted. These methods can be divided into three categories, that is, polymer entrapment, monomer polymerization, and particle swelling. The first involves the entrapment

*Corresponding author. Tel.: +86-22-2740-6590; fax: +86-22-2740-7957.

E-mail address: ysun@tju.edu.cn (Y. Sun).

0021-9673/01/$ – see front matter
PII: S0021-9673(01)00860-3

of magnetic materials with crosslinked polymers such as polysaccharides [8], polyvinyl alcohol [9] and proteins [10]. The second uses monomers such as styrene [11] and acrylamide [12] that can be initiated to polymerize around magnetic materials. Finally, the third approach is to swell compact or porous polymer particles with a solution of iron salts and then make the salts precipitate within the particles by raising the pH [13]. The monomer polymerization and particle swelling methods usually give more precise control in the shape and size of the resultant supports than the polymer entrapment method does. However, the preparation processes are complex and the polymer supports are often of poor biocompatibility. On the contrary, the polymer entrapment procedure is simple, and the final magnetic support obtained by this method usually exhibits good biocompatibility because polymers from natural sources are used.

Due to its high functionality and hydrogel-like properties, poly(vinyl alcohol) (PVA) appears to be an appropriate substitute for the commonly used natural materials such as agarose and serum albumin in the preparation of magnetic polymer supports [14]. In this work, PVA microspheres containing Fe_3O_4 colloidal particles have been prepared by an emulsification-crosslinking procedure. A reactive dye, Cibacron blue 3GA, was immobilized to the magnetic PVA gel as an affinity ligand. The resultant PVA-based magnetic affinity support (MAS) was then characterized by protein uptake equilibria and kinetics using lysozyme and bovine serum albumin as model proteins. A pore diffusion model and a homogeneous diffusion model were employed to simulate the uptake process of the proteins, and the application scope of the models has been discussed.

2. Materials and methods

2.1. Materials

PVA-1788 (M_r 74 800–79 200, 88% hydrolyzed) was from Beijing Organic Chemical Co. (Beijing, China), and PVA-2199 (M_r 89 000–98 000, 99% hydrolyzed) from Sigma–Aldrich (St. Louis, MO, USA). Antifoamer 7010 [poly(oxyethylene–oxypropylene) glycerol ether] was purchased from Tianjin Tianzhu Fine Chemicals (Tianjin, China). Vegetable oil was obtained from a local store. Surfactant Span 80 (sorbitan monooleate) was a product of Tianhai Fine Chemicals Co. (Tianjin, China). Cibacron blue 3GA (CB), lysozyme (chicken egg white) and bovine serum albumin (BSA) (fraction V, minimum 98%) were received from Sigma–Aldrich. Blue dextran (M_r $2 \cdot 10^6$) was purchased from Amersham Pharmacia Biotech (Uppsala, Sweden). All other reagents were of analytical grade and used as received. A neodymium-iron-boron permanent magnet (maximum field strength 0.4 Tesla) from the Research Institute of Rare Earth Elements (Baotou, China) was used to provide a necessary magnetic field for support separation.

2.2. Preparation of PVA-based magnetic affinity support

Four steps were required to prepare a PVA-based magnetic affinity support (MAS): (i) preparing a ferrofluid containing PVA-stabilized Fe_3O_4 colloidal particles; (ii) preparing microspheres entrapping Fe_3O_4 colloids and crosslinking with glutaraldehyde the PVA chains in the microspheres to form stable magnetic PVA beads; (iii) eliminating residual formyl groups on the support by reduction; and (iv) coupling CB to the support. In a previous report [15], we prepared a magnetic PVA gel by directly crosslinking the Fe_3O_4 colloidal particles in the ferrofluid, which involved the formation of irregular particles with a large size distribution. In the present work, we developed an emulsification-crosslinking method to prepare the magnetic PVA gel. Thus, except step (ii) in the preparation of magnetic PVA gel, all the other steps in the present work were exactly the same as those reported elsewhere [15]. Given below are the details for step (ii) and a brief description of the other three steps.

Step (i): A 30-ml volume of aqueous $FeCl_2$ solution (0.18 mol/l) was mixed with 40 ml of 50 g/l PVA-1788 at 50°C under nitrogen atmosphere. Three to six drops of antifoamer 7010 was introduced to prevent foam formation. Under vigorous agitation, 10 ml of 0.18 mol/l H_2O_2 and 20 ml of 3.0 mol/l NaOH were slowly added to the mixture in turn. The mixture was aged for 2 h at 50°C, and then cooled to ambient temperature. The magnetic fluid

thus obtained was dialyzed against water for 24 h and collected in a flask prior to the following crosslinking treatment.

Step (ii): A water-in-oil (W/O) emulsification-crosslinking method was used to prepare the magnetic PVA gel. The oil phase was made up by dissolving 15 g of Span 80 into 300 ml of vegetable oil. The aqueous phase was freshly prepared by mixing 10 ml of the ferrofluid with 10 ml of 100 g/l PVA-2199 solution and 0.5 ml of 50% (w/w) glutaraldehyde. The mixture was sonicated for 10 min to ensure a homogeneous dispersion of the magnetic colloidal particles. The two phases were then transferred into a 1-l stainless steel reactor equipped with an agitator and a water jacket. After circulating 60°C water through the jacket and agitating the two-phase mixture at 1400 rpm for 30 min, a stable W/O emulsion was formed. To the emulsion was dropwise added 5 ml of 0.5 mol/l hydrochloric acid, which catalyzed the crosslinking reaction between the hydroxyl groups on PVA chains and the formyl groups of glutaraldehyde. After 30 min, the reaction was terminated by introducing 2 ml of 3.0 mol/l NaOH to the mixture and cooling with tap water circulated to the water jacket. The magnetic PVA gel thus produced was recovered by centrifugation at 1600 *g* for 30 min and repeatedly washed with acetone, ethanol and water to clean the oil bound on its surface.

Step (iii): Formyl groups remaining on the magnetic PVA gel were reduced to hydroxyl groups by suspending about 5.0 g of the solid-phase in 100 ml of 0.1 mol/l $NaBH_4$ solution and shaking it overnight in a shaking incubator (160 rpm) at room temperature.

Step (iv): About 5.0 g of the reduced magnetic PVA gel was dispersed in 100 ml of 2 m*M* CB solution (pH 12), and the mixture was placed in an incubator of 25°C, shaking at 160 rpm for 24 h. The CB-modified magnetic support was routinely washed with deionized water, 25% (v/v) ethanol, and finally Tris–HCl buffer (0.01 mol/l, pH 7.6) to remove unbound CB. The coupling density of CB to the support was determined by mass balance.

2.3. Protein adsorption

Adsorption equilibria and kinetics of lysozyme and BSA to the MAS were examined using the batch adsorption method [15]. All the experiments were performed at 25°C in 0.01 mol/l Tris–HCl buffer (pH 7.6) containing a definite amount of NaCl. Pre-equilibrated with an appropriate buffer, the MAS was magnetically settled in a 10-ml graduated cylinder and the bed volume was measured (see below for the measurement of settled-bed voidage). It was then diluted with the buffer to give a suspension with known solid concentration (typically 1–2%, v/v). A 1–2 ml volume of the well-dispersed MAS suspension, 0–3 ml of protein solution (3 mg/ml), and fresh buffer (if necessary) were mixed in a 10-ml test tube to give a 5-ml mixture with a protein concentration of 0–1.8 mg/ml. In kinetic studies, up to ten tubes with identical mixture composition were prepared and shaken end to end in a laboratory rotator at 160 rpm for different periods of time (0–h). After that, the MAS was magnetically collected to the sidewall of the tube, and the supernatant was withdrawn for protein content measurement. In equilibrium studies, tubes with different protein content were incubated in the rotator for 6 h, which was confirmed by the results of kinetic studies to be sufficient to reach uptake equilibrium under all the conditions studied. Non-specific bindings of the proteins were tested using undyed magnetic PVA gel. The adsorbed protein density in terms of milligrams per ml of the magnetic PVA gel/MAS was calculated by mass balance [16].

2.4. Analysis and measurements

The particle size distribution of the MAS was measured with a Mastersizer 2000 unit (Malvern Instruments, UK) and the result is shown in Fig. 1. The measurement of packed-bed voidage and intraparticle porosity of the magnetic PVA gel was carried out on the Akta fast protein liquid chromatography (FPLC) system (Amersham Pharmacia Biotech, Uppsala, Sweden). The wet magnetic PVA gel was packed in a 50×5 mm I.D. column (HR5/5, Amersham Pharmacia Biotech), and 100-μl injections of blue dextran, acetone, lysozyme, and BSA were made to measure both the bed voidage and effective porosities of the support for different molecules. The packed-bed voidage and intraparticle porosities were determined using the chromatograph-

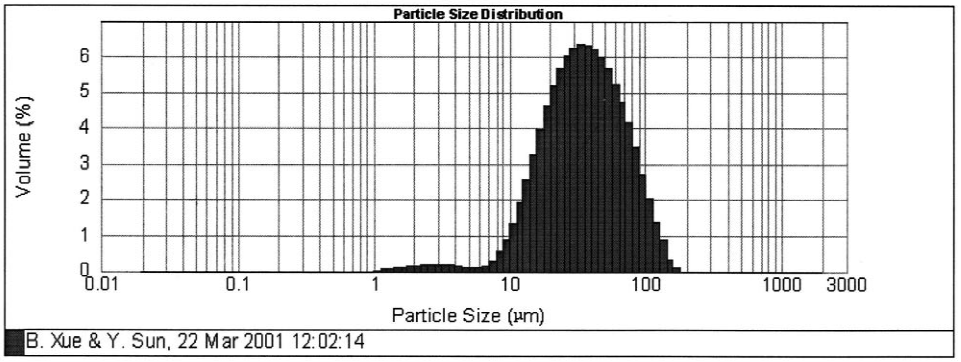

Fig. 1. Particle size distribution of MAS measured with a Mastersizer 2000 unit (Malvern Instruments).

ic retention data [17]. In order to eliminate non-specific binding of proteins to the undyed gel, Tris–HCl buffer containing 0.2 mol/l NaCl was used as the mobile phase (see below). The bed density was determined by weighting the column before and after the gel packing. The weight percentage of Fe_3O_4 in the support is calculated from the following equation:

$$Fe_3O_4\% = \frac{\rho_p - \rho_{gel}}{\rho_{Fe_3O_4} - \rho_{gel}} \cdot 100 \quad (1)$$

where $\rho_{Fe_3O_4}$ is the density of Fe_3O_4 ($5.18 \cdot 10^3$ kg/m^3, Ref. [18]), ρ_{gel} the density of PVA hydrogel (assumed to be $1.0 \cdot 10^3$ kg/m^3), ρ_p the density of drained MAS particles.

Concentrations of proteins and CB were measured with a UV–Vis spectrophotometer (752C, Shanghai Analytical Instrument Co., China) at 280 and 620 nm, respectively. The extinction coefficients determined by preliminary experiments were 2.245 l g^{-1} cm^{-1} for lysozyme, 0.633 l g^{-1} cm^{-1} for BSA and 12.35 mM^{-1} cm^{-1} for CB. These values were in agreement with those reported previously [19,20].

All the physical properties of the MAS are summarized in Table 1.

3. Kinetic models and simulations

There have been many investigations on the intraparticle transport of proteins, including linear driving force model [21], pore diffusion model (PDM) [22], homogeneous diffusion model (HDM) [23,24], surface diffusion model [25], and parallel diffusion model [26]. In this work, the uptake kinetics of the MAS is analyzed by the PDM and HDM, and results from the two models are compared.

Table 1
Physical properties of MAS

d_p (μm)	ε_b (−)		ρ_b (g/ml)	ρ_p (g/ml)	CB (μmol/ml)	Fe_3O_4 (wt%)	PVA (g/l)	ε_p (−)	$\varepsilon_{p,Lys}$ (−)	$\varepsilon_{p,BSA}$ (−)
42.6[a]	0.50[b]	0.39[c]	1.06[b]	1.12[d]	70[e]	2.6[f]	240[g]	0.81	0.51[h]	0.28[h]

[a] Volume-average diameter measured with a Mastersizer 2000 unit.
[b] Column packed by magnetic sedimentation.
[c] Column packed according to the manufacturer's instruction (Amersham Pharmacia Biotech).
[d] Calculated with the voidage and density of the packed bed.
[e] Calculated from mass balance of CB.
[f] Calculated from Eq. (1).
[g] PVA concentration in gel, measured with PVA gel free of magnetic material.
[h] Measured with undyed magnetic PVA gel according to their chromatographic retentions.

3.1. Pore diffusion model

This model assumes that the driving force for intraparticle mass transfer is protein concentration gradient in the pores of the adsorbent, and proteins adsorbed to the available binding sites within the pores remains fixed, that is, there exits no surface diffusion. The intraparticle continuity equation for the model is described as:

$$\left(\varepsilon_{p,e} + \frac{dq}{dc}\right) \cdot \frac{\partial c}{\partial t} = \frac{\varepsilon_{p,e} D_p}{r^2} \cdot \frac{\partial}{\partial r}\left(r^2 \cdot \frac{\partial c}{\partial r}\right) \quad (2)$$

The initial and boundary conditions are:

$$t = 0, \quad c = 0 \quad (2a)$$

$$r = 0, \quad \frac{\partial c}{\partial r} = 0 \quad (2b)$$

$$r = r_p, \quad \varepsilon_{p,e} D_p \cdot \frac{\partial c}{\partial r} = k_f (c_b - c|_{r=r_p}) \quad (2c)$$

where dq/dc is the slope of adsorption isotherm expressed on a whole particle volume basis (including the volume of the pores in the particle).

3.2. Homogeneous diffusion model

In the HDM, the adsorbent is considered as a homogeneous network, and the driving force is the total protein concentration gradient in the adsorbent. The intraparticle continuity equation for the model is:

$$\frac{\partial q}{\partial t} = \frac{D_e}{r^2} \cdot \frac{\partial}{\partial r}\left(r^2 \cdot \frac{\partial q}{\partial r}\right) \quad (3)$$

with the following initial and boundary conditions:

$$t = 0, \quad q = 0 \quad (3a)$$

$$r = 0, \quad \frac{\partial q}{\partial r} = 0 \quad (3b)$$

$$r = r_p, \quad D_e \cdot \frac{\partial q}{\partial r} = k_f (c_b - c|_{r=r_p}) \quad (3c)$$

3.3. Liquid phase mass transport

The mass transfer of protein from liquid phase to the solid-phase is expressed by:

$$\frac{dc_b}{dt} = -\frac{3 k_f H}{r_p} \cdot (c_b - c|_{r=r_p}) \quad (4)$$

The initial condition for this equation is as follows:

$$t = 0, \quad c_b = c_{b,0} \quad (4a)$$

The liquid film mass transfer coefficient, k_f, can be calculated from the following correlation [27]:

$$k_f = \frac{2 D_{AB}}{d_p} + 0.31 \cdot \left(\frac{\mu}{\rho D_{AB}}\right)^{-2/3} \left(\frac{\Delta\rho\, \mu g}{\rho^2}\right)^{1/3} \quad (5)$$

3.4. Method of numerical solution

Together with Eqs. (4) and (5), the governing equations of the PDM and HDM were both solved by the orthogonal collocation method [22]. The number of collocation points in the radial direction of the adsorbent was set at eight; further increase in the number gave little influence on the simulation results.

4. Results and discussion

4.1. Support preparation

The properties of thoroughly hydrolyzed (99% or higher) and partially hydrolyzed (80% or 88%) PVAs are different in their hydrophobicities. The former is more hydrophilic than the latter, and thus preferred as the base matrix of the MAS for protein adsorption; the latter, however, is more effective as a colloid stabilizer than the former [28]. This is the reason why two types of PVA products, i.e., PVA-1788 and PVA-2199, were utilized respectively in the preparations of ferrofluid and magnetic gel.

Since the crosslinking reaction between PVA and glutaraldehyde was completely inhibited by NaOH involved in the preparation of the ferrofluid, the aqueous mixture of PVA and glutaraldehyde kept stable at room temperature. That is, no gelation occurred before the emulsification experiment. However, adding sufficient HCl to the W/O emulsion initiated the crosslinking reaction effectively. It is an advantage of the emulsification-crosslinking method that the crosslinking reaction can be easily switched

on or off by adding concentrated acidic or basic solutions.

4.2. Properties of MAS

Microscopy observation showed that the support beads were nearly spherical, and only a small part of the beads were in the form of aggregates. These aggregates appeared at the later stage of the crosslinking step, when the viscosity of the aqueous phase was high enough to partly counteract the shear stress produced by agitation, and some of the liquid drops contacting with each other would not be separated effectively but bound by the crosslinking agent. Both the individual beads and the aggregates were mechanically and chemically stable. Fig. 2 shows the flow characteristics of the magnetic PVA gel column. It can be seen that the gel packed column could endure a superficial liquid flow-rate of up to 400 cm/h. Another feature of the magnetic PVA gel is that it could readily be re-dispersed after magnetic separations or chromatographic operations at 2.8 MPa. Further agglomeration of the individual beads and the aggregates due to the stickiness of PVA, as has been reported by Wu and Wisecarver [29], was not observed. The magnetic PVA gel was very stable in a pH range of 2–14. It could not be digested with concentrated HCl or NaOH solution, so the ligand density of the MAS was measured by mass balance instead of the commonly used peptization method [16].

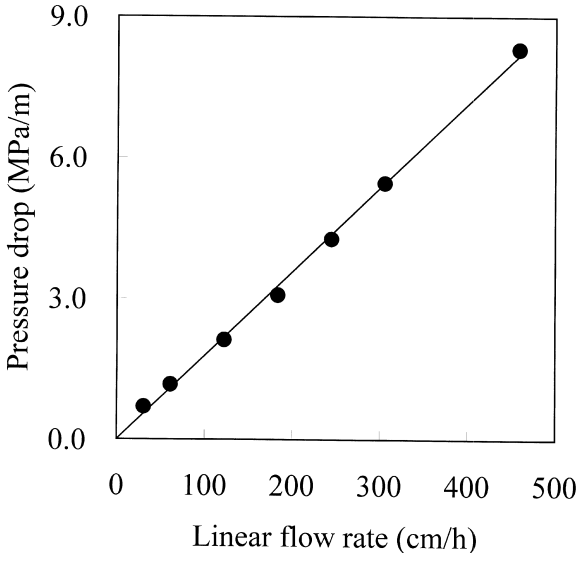

Fig. 2. Flow characteristics of column packed with magnetic PVA gel. The measurement was carried out with a 50×5 mm I.D. column.

The Fe_3O_4 content of the MAS, 2.6% (Table 1), is sufficiently high to realize rapid separation of the MAS in a magnetic field. In the adsorption studies, the MAS could be separated from the protein-support suspension in less than 10 s simply with the hand-held magnet. The high efficiency in magnetic separation ensured the reliability of the kinetic data discussed below.

For high molecular mass adsorbates such as proteins, the effective porosity of the adsorbent usually decreases as the molecular mass of the proteins increases. The effective porosities obtained in the present work obey this rule (Table 1). It is notable that the PVA concentration in the support, 240 g/l (Table 1), was higher than the initial PVA concentration in the water phase in preparation (about 50 g/l). This might be due to the shrinkage of the support during the crosslinking step, in which excessive water was squeezed out. The concentration effect resulted in a dense PVA network with relatively small effective porosities for proteins. As a comparison, the effective porosities in Sepharose CL-6B, a 6% crosslinked agarose gel, are 0.73 for lysozyme and 0.55 for BSA [17]. The presence of non-porous Fe_3O_4 particles in the MAS can hardly affect its effective porosity because the volume percentage of Fe_3O_4, which was calculated from the weight percentage of Fe_3O_4, is less than 0.5%.

4.3. Adsorption equilibria

The adsorption isotherms of lysozyme and BSA to the MAS and the undyed magnetic gel are presented respectively in Figs. 3 and 4. The adsorption of lysozyme to the dyed support is very favorable at low salt concentration, and becomes less favorable as the salt concentration is increased. In both cases, the experimental data can be well fitted by the Langmuir isotherm (Eq. (6)). In contrast, the adsorption of BSA obeys the Henry's law (Eq. (7)), as reported in the previous publication [15]:

$$q = \frac{q_m c}{K_c + c} \tag{6}$$

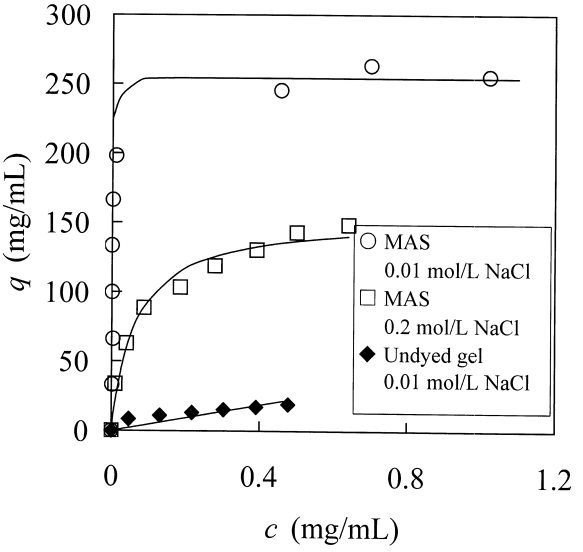

Fig. 3. Adsorption isotherms of lysozyme to both MAS and undyed gel under different ionic strength.

$$q = kc \tag{7}$$

The fitted parameters for these two kinds of isotherms are summarized in Table 2. Due to the high CB-substituting degree (Table 1), the binding capacity for lysozyme is more than twice that of blue

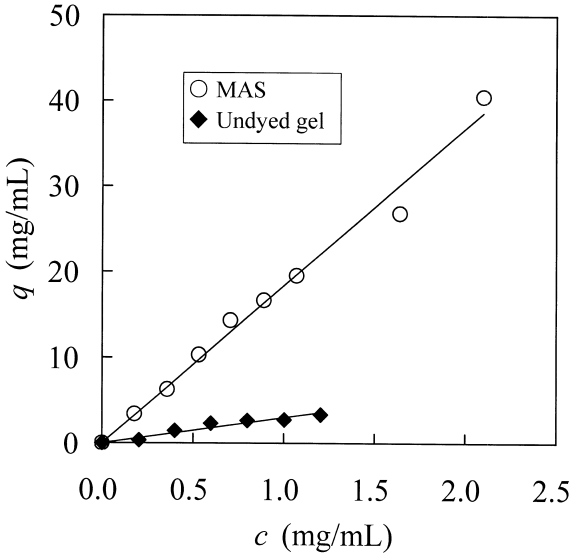

Fig. 4. Adsorption isotherms of bovine serum albumin to both MAS and undyed gel at an ionic strength of 0.01 mol/l.

Table 2
Parameters for adsorption isotherms

[NaCl] (mol/l)	Lysozyme (Eq. (6))		BSA (Eq. (7))
	q_m (mg/ml)	K_d (mg/ml)	k (−)
0.01	254	0.0035	18.4
0.2	154	0.063	Not determined

Sepharose [19]. The isotherms for the undyed gel are both linear and very flat, indicating that the contribution of nonspecific binding to the total capacity of the MAS is small.

The effect of ionic strength on protein adsorptions was also investigated (Fig. 5). As expected, the adsorption ability of the MAS is suppressed at higher ionic strength, which is in agreement with previous publications [16,19]. This phenomenon is due to the hydrophobic interaction between the ligands and the base matrix of the support, which increases with ionic strength and thus reduces the number of ligands accessible to proteins [30]. The adsorption of the proteins to the undyed gel is also sensitive to the ionic strength and can completely be inhibited at a NaCl concentration of 0.2 mol/l or higher. This feature makes it feasible to measure the effective porosities by the chromatography method described in Section 2.4.

4.4. Adsorption kinetics

Table 3 lists the experimental conditions in the kinetic studies and the fitted parameters by the two kinetic models. The solid lines in Fig. 6 are calculated from the PDM, while the dashed lines are from the HDM (only the dashed line for Run 1 is visible, others are completely overlapped with the solid lines). The overlap of the curves reflects the intrinsic relationship of D_p and D_e. Combining the linear isotherm of BSA (Eq. (7)) and considering that $\varepsilon_{p,BSA} \ll k$, Eq. (2) can be rewritten as:

$$\frac{\partial q}{\partial t} = \left(\frac{\varepsilon_{p,BSA} D_{p,BSA}}{\varepsilon_{p,BSA} + k}\right) \cdot \frac{1}{r^2} \cdot \frac{\partial}{\partial r}\left(r^2 \cdot \frac{\partial q}{\partial r}\right) \approx \left(\frac{\varepsilon_{p,BSA} D_{p,BSA}}{k}\right) \cdot \frac{1}{r^2} \cdot \frac{\partial}{\partial r}\left(r^2 \cdot \frac{\partial q}{\partial r}\right) \tag{8}$$

Eq. (8) indicates that in the case of BSA adsorption,

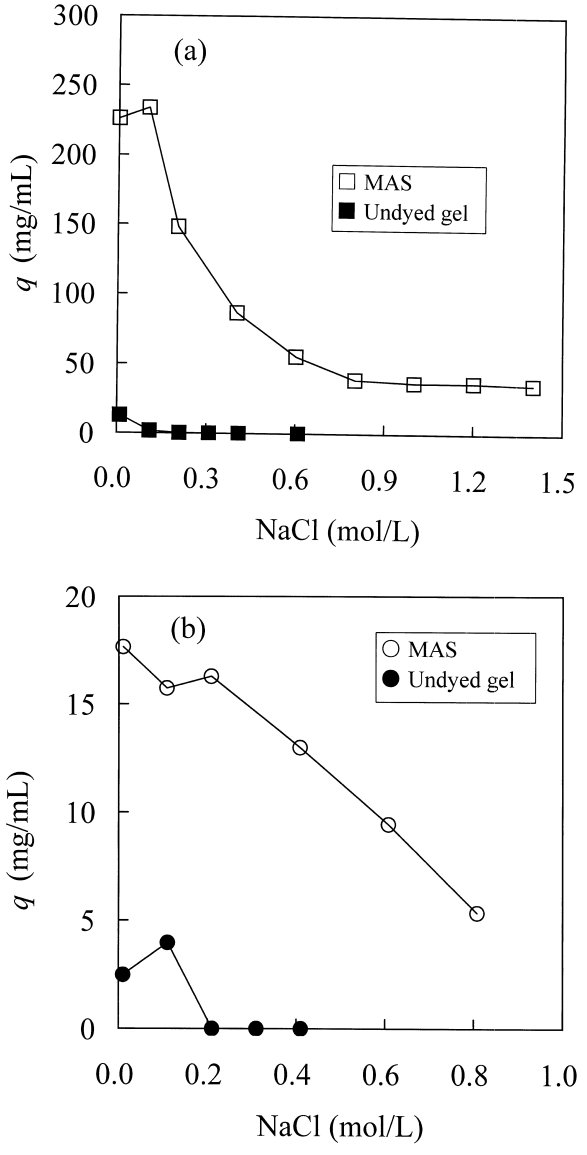

Fig. 5. Effect of ionic strength on the adsorption of (a) lysozyme and (b) bovine serum albumin to both MAS and undyed gel. Initial protein concentration ($c_{b,0}$) was 1.2 mg/ml. The volumetric ratio of solid to liquid in the reaction mixture (H) was 0.006.

the PDM is just identical to the HDM, and the two diffusivities are correlated by:

$$D_{e,BSA} = \frac{\varepsilon_{p,BSA} D_{p,BSA}}{k} \quad (9)$$

In the case of lysozyme adsorption, D_e and D_p cannot be easily correlated because of its nonlinear isotherm (Eq. (6)). As an approximation, an average slope is defined as [26]:

$$S_{av} = \frac{\int_0^{c_{b,0}} \frac{dq}{dc}\, dc}{\int_0^{c_{b,0}} dc} = \frac{q_0}{c_{b,0}} = \frac{q_m}{K_d + c_{b,0}} \quad (10)$$

The calculated average slopes are 421 for Run 1 and 232 for Run 2. The effective diffusivity and the pore diffusivity of lysozyme are thus correlated by:

$$D_{e,Lys} = \frac{\varepsilon_{p,Lys} D_{p,Lys}}{S_{av}} \quad (11)$$

In Fig. 7 is shown the difference between the fitted D_e values in Table 3 and those calculated from Eqs. (9) and (11). It can be seen that the approximation for Run 1 is not very good because the isotherm is nearly rectangular (see Fig. 3). For the less favorable isotherm under higher ionic strength (Run 2), however, the approximation is quite satisfactory. These results account for why in Fig. 6 the dashed line for Run 2 overlaps with the solid line, while that for Run 1 does not.

If the product of $\varepsilon_{p,e}$ and D_p in Eq. (2) is treated as a single parameter, its value would be insensitive to the change of $\varepsilon_{p,e}$ because dq/dc is usually much greater than $\varepsilon_{p,e}$, as is in this work. Thus, many researchers use ε_p rather than $\varepsilon_{p,e}$ on the left-hand side of Eq. (2) and a single effective pore diffusivity, $D_{p,e}$, rather than $\epsilon_{p,e} D_p$ on the right-hand side [23,31]. To make reasonable comparisons of the intraparticle mass transfer characteristics of the MAS with other adsorbents, the values of $\varepsilon_{p,e} D_p$ are also calculated and listed in Table 3.

Miyabe and Guiochon [31] has reported the mass transfer of BSA in two anion-exchangers; the $D_{p,e}$ values (equivalent to $\varepsilon_{p,e} D_p$) ranged from $1.3 \cdot 10^{-11}$ to $2.4 \cdot 10^{-11}$ m^2/s in Source-Q and from $1.3 \cdot 10^{-12}$ to $2.3 \cdot 10^{-12}$ m^2/s in TSK-GEL-DEAE-5PW. He et al. reported that the $D_{p,e}$ of BSA in blue Sepharose was $1.8 \cdot 10^{-12}$ m^2/s [22]. The $D_{p,e}$ values of lysozyme in Poros 50 HS [23], a rigid macroporous resin, and in Streamline SP [24] were $1.0 \cdot 10^{-11}$ m^2/s and $3.5 \cdot 10^{-11}$ m^2/s, respectively. These results indicate that $D_{p,e}$ obtained with different proteins and different adsorbents may vary greatly due to the different shapes and sizes of both the proteins

Table 3
Experimental and kinetic parameters related to dynamic uptake simulations

Run No.	Protein	Experimental conditions			Diffusivities (m^2/s)			
		$c_{b,0}$ (mg/ml)	H (−)	[NaCl] (mol/l)	D_{AB} ($\times 10^{-11}$)	D_p ($\times 10^{-12}$)	D_e ($\times 10^{-15}$)	$\varepsilon_{p,e}D_p$ ($\times 10^{-12}$)
1	Lys	0.60	0.003	0.01	13.4[a]	8.0	6.0	4.1
2		0.60	0.003	0.20		15.0	33.0	7.7
3	BSA	0.86	0.018	0.01	6.7[a]	0.65	10.0	0.18
4		1.20	0.006	0.01		0.65	10.0	0.18

[a] Data from Ref. [35] and adjusted to 25°C according to the Stokes–Einstein equation. k_f are $1.5\cdot10^{-5}$ m/s for lysozyme and $8.8\cdot10^{-6}$ m/s for BSA, calculated from Eq. (5).

and the pores in the adsorbents. In this work, the $\varepsilon_{p,e}D_p$ values for lysozyme and BSA are about one tenth to a half those in the above-mentioned adsorbents. Since the binding rate of proteins to affinity ligands is very high [32] and protein-dye binding can reach equilibrium instantaneously [33], the adsorption kinetics of the present system is considered to be an intraparticle diffusion controlling process. Therefore, the smaller values of the $\varepsilon_{p,e}D_p$ in the present system than those in other adsorbents are considered due to the high PVA concentration in the MAS, which resulted in higher hindrance to protein diffusion.

Furthermore, due to the highly hindered diffusion of the proteins in the MAS, the external film mass transfer resistance was negligible. Thus, the PDM and HDM can be simplified by omitting the external film mass transfer. It is supported by the agreement between the simulation results obtained from the original and simplified models (simulation data not shown).

Liapis has assumed that surface diffusion of proteins within porous affinity adsorbents can be

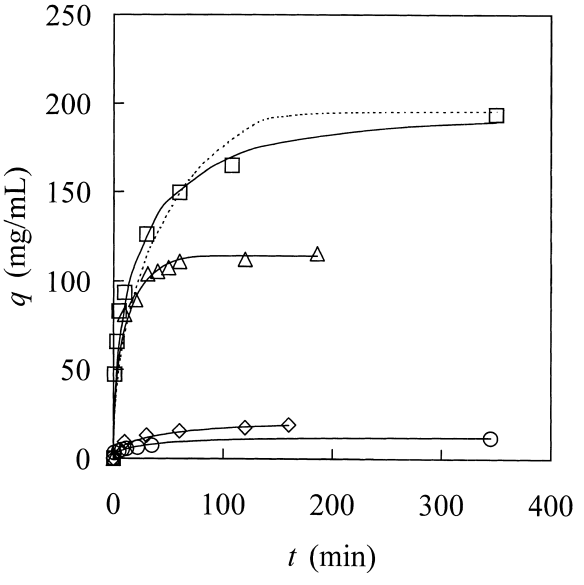

Fig. 6. Adsorption kinetics of lysozyme and bovine serum albumin to MAS. Scattered plots represent the experimental data of (□) Run 1, (△) Run 2, (○) Run 3 and (◇) Run 4. The experimental conditions for different Runs are listed in Table 3. The solid lines are calculated from the PDM, and the dashed lines are from the HDM, which overlaps with the solid lines for Runs 2 to 4.

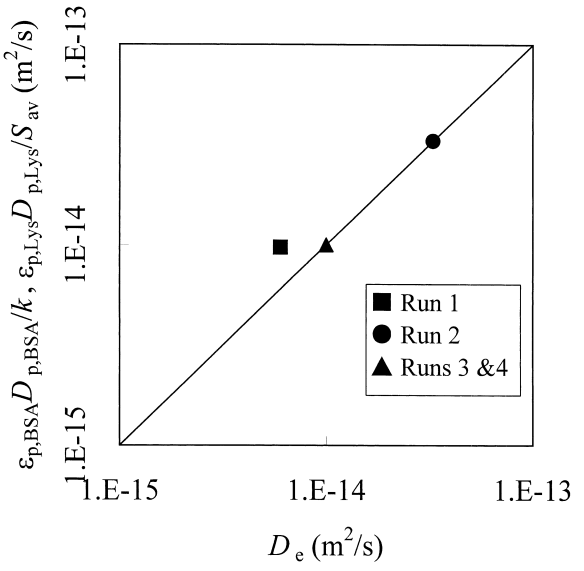

Fig. 7. Comparison of homogenous diffusivities obtained by data fitting with those calculated from Eqs. (9) and (11).

neglected due to the strong interaction between proteins and affinity ligands [34]. According to the isotherm parameters in Table 2, the interaction between lysozyme and CB at low ionic strength can be regarded as strong (the isotherm is nearly rectangular), but the same conclusion can not be drawn for lysozyme–CB interactions at high ionic strength and for BSA–CB interactions. In other words, surface diffusion in Runs 2 to 4 cannot be neglected. In this case, the D_p in the PDM is no longer a parameter that merely characterize the diffusion of proteins in the pores, but rather a parameter that reflects the parallel contributions of pore diffusion and surface diffusion [31]. This explains why the PDM gives good fittings for both the cases of pore diffusion dominant (Run 1) and parallel diffusion (Runs 2 to 4). The positive dependence of $D_{p,Lys}$ on ionic strength (see Table 3) is quite understandable, since the interaction between lysozyme and CB is weakened at higher ionic strength and, as a result, the surface diffusion of lysozyme is promoted.

Different from the PDM, the HDM is suitable for the case where surface diffusion controls the mass transfer [26]. Therefore, its fitting for Run 1 is poor. However, when the contribution of surface diffusion becomes significant, as is in Runs 2 to 4, it can gives fittings as good as those given by the PDM (Fig. 6).

5. Conclusions

A micron-sized magnetic PVA gel has been synthesized by an emulsification-crosslinking method, and a MAS was prepared by coupling Cibacron blue 3GA to the magnetic gel. The MAS showed high mechanical and chemical stabilities and magnetic responsiveness. The adsorption properties of the magnetic affinity support were tested using lysozyme and BSA as model proteins. The adsorption of lysozyme was favorable, and the adsorption capacity of lysozyme reached up to 254 mg/ml, more than two times higher than commercially available blue agarose gel. The adsorption of BSA obeys the Henry's law with a Henry's constant of 18.4. Adsorption kinetics of the two proteins to the MAS was studied with two diffusion models, and the results show that the mass transfer within the MAS is slower when compared with some commonly used commercial adsorbents. This phenomenon is attributed to the relatively high PVA concentration in the support, which leads to a PVA gel with small meshes and thus great hindrance to protein diffusion. Simulation of the uptake kinetics of these proteins shows that for lysozyme with a rectangular isotherm, the pore diffusion model is preferred because the pore diffusion is dominant in intraparticle mass transfer. In the case of lysozyme with less favorable isotherm at higher ionic strength, both the models are applicable. For BSA with a linear isotherm, the two models are essentially identical, and D_p is proportional to D_e by a simple relationship.

6. Nomenclature

c	Means protein concentration (mg/ml)
d_p	Means mean particle diameter (m)
D_e	Means effective diffusivity in homogeneous diffusion model (m^2/s)
D_p	Means pore diffusivity in pore diffusion model (m^2/s)
$D_{p,e}$	Means effective pore diffusivity (m^2/s)
D_{AB}	Means diffusivity in free solution (m^2/s)
H	Means volumetric ratio of support (solid-phase) to solution (liquid phase)
k	Means parameter for Henry's isotherm
k_f	Means liquid film mass transfer coefficient (m/s)
K_d	Means dissociation constant for Langmuir isotherm (mg/ml)
q	Means adsorbed protein density (mg/ml)
$q_0 q$	Means in equilibrium with $c_{b,0}$ (mg/ml)
q_m	Means adsorption capacity for Langmuir isotherm (mg/ml)
r_p	Means mean particle radius (m)
R	Means normalized particle radius
t	Means time (min)
ε_p	Means particle porosity towards small molecules
$\varepsilon_{p,e}$	Means effective particle porosity to proteins
$\varepsilon_{p,Lys}$	Means effective particle porosity to lysozyme
$\varepsilon_{p,BSA}$	Means effective particle porosity to BSA
μ	Means liquid viscosity (kg/m/s)
ρ	Means liquid density (kg/m^3)

ρ_{gel} Means density of PVA hydrogel, assumed to be $1.0 \cdot 10^3$ kg/m^3

ρ_p Means density of drained MAS particles, $1.12 \cdot 10^3$ kg/m^3

$\Delta\rho$ Means density difference between solid support and liquid phase (kg/m^3)

Acknowledgements

This work was supported by the National Natural Science Foundation of China (grant No. 20025617).

References

[1] H. Bierau, Z. Zhang, A. Lyddiatt, J. Chem. Technol. Biotechnol. 74 (1999) 208.
[2] R. Hjorth, Trends Biotechnol. 15 (1997) 230.
[3] I. Safarik, M. Safarikova, J. Chromatogr. B Biomed. Sci. Appl. 722 (1999) 33.
[4] Z. Zhang, D.A. O'Sullivan, A. Lyddiatt, J. Chem. Technol. Biotechnol. 74 (3) (1999) 270.
[5] R.R. Dauer, E.H. Dunlop, Biotechnol. Bioeng. 37 (1991) 1021.
[6] R. Hartig, M. Hausmann, G. Luers, M. Kraus, G. Weber, C. Cremer, Rev. Sci. Instrum. 66 (5) (1995) 3289.
[7] C.B. Fuh, S.Y. Chen, J. Chromatogr. A 857 (1999) 193.
[8] P.R. Levison, S.E. Badger, J. Dennis, P. Hathi, M.J. Davies, I.J. Bruce, D. Schimkat, J. Chromatogr. A 816 (1998) 107.
[9] C. Bergemann, D. Muller-Schulte, J. Oster, L.A.S. Brassard, J. Magn. Magn. Mater. 194 (1999) 45.
[10] M. Koneracka, P. Kopcansky, M. Antalik, M. Timko, C.N. Ramchand, D. Lobo, R.V. Mehta, R.V. Upadhyay, J. Magn. Magn. Mater. 201 (1999) 427.
[11] K. Furusawa, K. Nagashima, C. Anzai, Colloid Polym. Sci. 272 (1994) 1104.
[12] T.M. Cocker, C.J. Fee, R.A. Evans, Biotechnol. Bioeng. 53 (1997) 79.
[13] J. Ugelstad, T. Ellingsen, A. Berge, O.B. Helgee, Pat. US 4 654 267 (1987).
[14] D. Muller-Schulte, F. Fusslde, M. Cuyper, in: U. Hafeli (Ed.), Scientific and Clinical Applications of Magnetic Carriers, Plenum Press, New York, 1997, p. 93.
[15] B. Xue, X.D. Tong, Y. Sun, Sep. Sci. Technol. (in press).
[16] L.Z. He, Y.R. Gan, Y. Sun, Bioprocess Eng. 17 (1997) 301.
[17] P.M. Boyer, J.T. Hsu, AIChE J. 38 (1992) 259.
[18] R.C. Weast (Ed.), CRC Handbook of Chemistry and Physics, CRC Press, Boca Raton, FL, 1988.
[19] P.M. Boyer, J.T. Hsu, Chem. Eng. Sci. 47 (1992) 241.
[20] A. Compagninni, S. Fisichella, S. Foti, J. Chromatogr. A 736 (1996) 115.
[21] H.S. Tsou, E.E. Graham, AIChE J. 31 (1985) 1959.
[22] L.Z. He, X.Y. Dong, Y. Sun, Biochem. Eng. J. 2 (1998) 53.
[23] L.E. Weaver Jr., G. Carta, Biotechnol. Prog. 12 (1996) 342.
[24] P.R. Wright, F.J. Muzzio, B.J. Glasser, Biotechnol. Prog. 14 (1998) 913.
[25] R.D. Tilton, C.R. Robertson, A.P. Gast, J. Colloid. Interf. Sci. 137 (1990) 192.
[26] H. Yoshida, M. Yoshikawa, T. Kataoka, AIChE J. 40 (1994) 2034.
[27] B.J. Horstmann, H.A. Chase, Chem. Eng. Res. Des. 67 (1989) 243.
[28] M.K. Lindemann, in: N.M. Bikales (Ed.), Encyclopeida of Polymer Science and Technology, Interscience, New York, 1971, p. 149.
[29] K.Y.A. Wu, K.D. Wisecarver, Biotechnol. Bioeng. 39 (1992) 447.
[30] Y.C. Liu, E. Stellwagen, J. Biol. Chem. 262 (1987) 583.
[31] K. Miyabe, G. Guiochon, J. Chromatogr. A 866 (2000) 147.
[32] W.C. Olson, M.L. Yarmush, Biotechnol. Prog. 3 (1987) 177.
[33] B. Champluvier, M.R. Kula, Biotechnol. Bioeng. 40 (1992) 33.
[34] A.I. Liapis, Sep. Purif. Methods 19 (1990) 133.
[35] M.T. Tyn, T.W. Gusek, Biotechnol. Bioeng. 35 (1990) 327.